

Effects of Right-handed Gauge Bosons in B - \bar{B} Mixing and CP Violation

Dennis Silverman

Department of Physics and Astronomy, University of California, Irvine, CA 92697-4575

W. K. Sze and Heng Yao

Department of Physics, National Taiwan Normal University, Taipei, Taiwan 117

(Dated: October 16, 2018)

In the Left-Right Symmetric Model (LRSM), box diagrams involving the charged right-handed gauge boson W_R may affect B - \bar{B} mixing as well as CP asymmetries in neutral B decays. The smallness of the ϵ_K parameter in the neutral K -meson system places severe constraints on the right-handed quark mixing matrix V^R , and reduces the number of its effective phases to one. W_R exchange gives a large contribution to B - \bar{B} mixing when the mass of the W_R boson is up to or higher than 8 TeV, depending on the V^R case, the $B_{d,s}$ meson, and the asymmetry. The allowed regions of the CP violating asymmetries $\sin 2\beta$, $\sin \gamma$, $\sin 2\alpha$, and $\sin 2\phi_s$, as well as x_s , are calculated as a function of the W_R mass. The results of the LRSM other than for the well measured $\sin 2\beta$ show allowable regions that are much broader than that for the Standard Model, showing that new experiments can indicate a presence of new physics, or significantly push up the limits on the W_R mass.

PACS numbers: 11.30Er, 12.15.Hh, 12.60.Cn, 14.65.Fy, 14.40.Nd.

Keywords: B - \bar{B} mixing, CKM matrix, beyond the standard model, W_R boson, CP asymmetry, B factories.

I. INTRODUCTION

The Standard Model (SM) for strong and electroweak interactions has achieved great success in explaining interactions among the elementary particles. Nonetheless, it is generally speculated that we may encounter richer symmetry structures, such as supersymmetry or larger gauge groups, as we go to higher energy scales. For example, in the Left-Right Symmetric Model (LRSM) [1], the right-handed quarks have gauge interactions among themselves, just like their left-handed counterparts, and such interactions have not yet been seen only because they are spontaneously broken at an energy higher than the electroweak scale. By examining such extended models to the SM, we may get a better understanding of the mixing and mass scales whose values are not restricted by any principle we know so far.

CP violation is an excellent realm to look for experimental effects of the LRSM, because the right handed mixings in LRSM bring in another 3×3 quark mixing matrix V^R which has new phases that can affect CP violation. We will see that constraints reduce the number of effective new phases to one in the B_d or B_s systems.

The main experimental data giving or constraining CP violation are listed in Table I [2]. Among the data listed in Table I, the ϵ_K parameter in the neutral K meson system has been known for a long time, and until recently was the only direct evidence for CP violation. With the advent of B factories, it is now possible to investigate CP violating effects in the neutral B meson system as well. Carter and Sanda [3] proposed that CP violating effects in B_q - \bar{B}_q ($q = d, s$) mixing can be probed by investigating decays of $B_q(\bar{B}_q)$ to a CP eigenstate f . The time-dependent CP asymmetries would show an oscillatory behavior, with a characteristic amplitude \mathcal{A}_f .

TABLE I:

Experiments and values constraining V	
$ V_{ub} $	$(3.6 \pm 0.7) \times 10^{-3}$
$ V_{cb} $	$(41.2 \pm 2.0) \times 10^{-3}$
$ \epsilon_K $	$(2.282 \pm 0.017) \times 10^{-3}$
ΔM_{B_d}	$0.502 \pm 0.006 \text{ ps}^{-1}$
x_s	> 19.0 at 95% CL
$\sin 2\beta$	0.735 ± 0.056

For example, in the decay $B \rightarrow J/\psi K_S$, the asymmetry $\mathcal{A}_{\psi K} = \sin 2\beta$ in the SM.

In this paper we investigate the possibility of larger ranges for these CP violating asymmetries in processes involving W_R bosons and V^R mixing in the LRSM. We use two models for the right handed coupling matrix which allow large couplings for box diagrams with two t quark sides containing one W_R and one W_L exchange, allowing effects in B_s mesons (case I), or B_d mesons (case II). For B_s mesons, the t quark right hand couples to s as well as to b quarks (case I), but does not also couple to d quarks, in order to minimize the right handed effects in K meson mixing or ϵ_K . For B_d mesons, the t quark right hand couples to d as well as to b quarks (case I), but not also to s quarks, in order to minimize the effect in ϵ_K . Although several phases and one mixing angle are present in each case, there is only one phase combination which contributes to CP violating asymmetries, and we vary it over all values.

We find significant effects from box diagrams containing both W_L and W_R exchanges for the W_R mass up to 8 TeV or higher, for both coupling cases I and II. Experiments on the CP violating asymmetries and on x_s may

find results outside the SM range, which would indicate new physics, such as the LRSM.

In the next section we will give a brief review of CP violation in the SM, and then in Sec. III of mixing in the LRSM, and describe its implication for neutral B meson physics. Apparently there are a few phases in the right-handed quark mixing matrix V^R which can contribute to CP violation in the B sector, but the constraints imposed by ϵ_K reduce the number of effective phases to only one, as discussed in Sec. IV. The effects of W_R on B - \bar{B} mixing is given in Sec. V, and its magnitudes shown in Sec. VI. Effects of W_R on specific CP violating asymmetries of $\sin 2\beta$, $\sin \gamma$, $\sin 2\alpha$, and $\sin 2\phi_s$ are presented in Sections VII, VIII, IX, and X, respectively. x_s is covered in Section XI, and the conclusions are summarized in Section XII.

II. CP VIOLATION IN THE STANDARD MODEL

In the SM with three generations of quarks, all CP -violating effects come from the 3×3 left-handed quark mixing matrix $V \equiv V^L$ (the CKM matrix) [4]. There are many possible ways to parameterize the phases appearing in V , but there is only one single independent re-parameterization invariant measure. For example, in Wolfenstein's parameterization [5]:

$$V = \begin{pmatrix} 1 - \frac{1}{2}\lambda^2 & \lambda & A\lambda^3(\rho - i\eta) \\ -\lambda & 1 - \frac{1}{2}\lambda^2 & A\lambda^2 \\ A\lambda^3(1 - \rho - i\eta) & -A\lambda^2 & 1 \end{pmatrix}. \quad (1)$$

the CP violating phases are assigned to the smallest elements $V_{ub} \equiv |V_{ub}|e^{-i\gamma}$ and $V_{td} \equiv |V_{td}|e^{-i\beta}$, and therefore, the phase angles β and γ can be sizable in spite of the tiny intrinsic CP violation. The CP violating parameter can then be taken as the area of the (d - b) unitarity triangle, which is half of Jarlskog's parameter J [6].

The parameter $\lambda \equiv |V_{us}| = 0.221$ in Eq. (1) is quite accurately known, and we will disregard its small uncertainty in subsequent analysis. The other three parameters are presently known, with larger uncertainties, to be of order 1.

On the other hand, if we normalize the base of the unitarity triangle to unit length, as is usually done, the other two sides of the triangle would be given by $|V_{ub}|/\lambda|V_{cb}|$ and $|V_{td}|/\lambda|V_{cb}|$, with β and γ as their respective opposite angles. Thus the first four data listed in Table I were sufficient to give estimates for the angles β and γ . Values of $\sin 2\beta$ obtained by earlier theoretical analyses were

$$\sin 2\beta = \begin{cases} 0.75 \pm 0.06 & [7], \\ 0.73 \pm 0.20 & [8]. \end{cases} \quad (2)$$

The experimental value of $\mathcal{A}_{\psi K}$ can then be compared with these theoretical predictions.

Measurements of the CP violating asymmetry in the decay $B \rightarrow J/\psi K_S$ now exist to high precision. The values obtained by BaBar [9], Belle [10], and CDF [11] are

$$\mathcal{A}_{\psi K} = \begin{cases} 0.741 \pm 0.067 \pm 0.034 & (\text{BaBar}), \\ 0.719 \pm 0.074 \pm 0.035 & (\text{Belle}), \\ 0.79 \pm 0.42 & (\text{CDF}). \end{cases} \quad (3)$$

These give the world-averaged value

$$\mathcal{A}_{\psi K} = 0.735 \pm 0.056. \quad (4)$$

We see that there is excellent agreement between Eq. (2) and Eq. (4). Besides β , the SM also has definite predictions for other CP violating asymmetries.

III. THE LEFT-RIGHT SYMMETRIC MODEL

In the LRSM, one assumes that the Lagrangian for the elementary particles obeys (apart from the $SU(3)_c$ for strong interaction) an $SU(2)_L \times SU(2)_R \times U(1)_{B-L}$ symmetry which is spontaneously broken at a scale v' to the electroweak gauge group $SU(2)_L \times U(1)_Y$. There would appear extra charged gauge bosons W_R^\pm which mediate coupling with strength g_R to the right-handed quarks. The mixing matrix V^R among the latter is in general different from V^L . For models which are relevant to hadron-scale physics, v' would not be much higher than the electroweak scale $v = 250$ GeV, so that the W_R mass $M_R = \frac{1}{2}g_R v'$ would not be too large either. Beall, Bander, and Soni [12] showed that with the manifest LR symmetry mixing matrix of $V^R = V^L$ that the mass of the W_R must exceed 1.6 TeV to not overly affect ΔM_K . We have calculated that satisfying the constraints of Table I with manifest LR symmetry gives a 2 - σ lower limit on M_R of 1.5 TeV. Olness and Ebel [13] pointed out that W_R can have sub-TeV mass if V^R takes on some specific forms. The detailed analysis of Langacker and Sankar [14] led to a similar conclusion, namely, that M_R can attain a lower limit of about 300 GeV if V^R assumes one of the following two forms:

$$V_I^R = e^{i\omega} \begin{pmatrix} 1 & 0 & 0 \\ 0 & ce^{i\tau} & se^{i\sigma} \\ 0 & -se^{i\phi} & ce^{i\chi} \end{pmatrix}, \quad (5a)$$

$$V_{II}^R = e^{i\omega} \begin{pmatrix} 0 & 1 & 0 \\ ce^{i\tau} & 0 & se^{i\sigma} \\ -se^{i\phi} & 0 & ce^{i\chi} \end{pmatrix} = V_I^R \begin{pmatrix} 0 & 1 & 0 \\ 1 & 0 & 0 \\ 0 & 0 & 1 \end{pmatrix}, \quad (5b)$$

where for brevity we denote $s \equiv \sin \theta_R$ and $c \equiv \cos \theta_R$. In what follows, the cases where $V^R = V_I^R$ and $V^R = V_{II}^R$ will be denoted as case I and case II, respectively. Unitarity of V^R implies that

$$\tau + \chi = \phi + \sigma \quad (6)$$

for both cases.

It has been pointed out that both cases for V^{R} can lead to sizeable contributions to CP violations for K and B mesons [15]. For the neutral B mesons, deviation from SM predictions can occur through modified B - \bar{B} mixing effects, where we have additional box diagrams with one W_L and one W_R exchange [16]. In what follows, we will examine how these ‘‘indirect’’ effects gives the corrections to SM predictions for the K - \bar{K} and B - \bar{B} systems. While direct CP violating effects involve long distance effects and final state interactions which are not very well understood, the long distance effects in box diagrams have been extensively studied by various groups with methods such as the $1/N$ expansion or lattice gauge calculations, and are conveniently summarized in terms of the so-called bag-parameters.

It is clear from Eqs. (5) that interchanging the roles played by d_R and s_R means swapping V_I and V_{II} . Specifically, since V_I has non-zero mixing angle factors in the second and third (s and b) columns only, we expect that

case I will give substantial corrections to the SM prediction for the B_s - \bar{B}_s system, but not for the B_d - \bar{B}_d one. The reverse is true for case II. These matrices can also be derived if one first looks for those with large right handed coupling of t or c quarks in box diagrams of mixings for B_d or B_s , and then constrains them to not have right handed t or c couplings in ϵ_K . The u quark right handed couplings do not count in the B systems, due to the small u quark mass, and are conveniently left out of the mixing matrix except where needed for unitarity.

IV. CONSTRAINTS FROM THE ϵ_K PARAMETER

The parameter ϵ_K for CP violations in the K - \bar{K} system is given as $\epsilon_K \approx \text{Im}\langle K^0 | H_{\Delta S=2} | \bar{K}^0 \rangle / \sqrt{2} \Delta m_K$. In the SM, the operator $H_{\Delta S=2}$ is given by the box diagrams with W_L - W_L exchanges [17]:

$$H_{\Delta S=2} = \frac{G_F^2 M_L^2}{4\pi^2} [\eta_{cc} S(x_c) \zeta_c^2 + \eta_{tt} S(x_t) \zeta_t^2 + 2\eta_{ct} S(x_c, x_t) \zeta_c \zeta_t] (\bar{d}_L s_L) (\bar{d}_L s_L) + \text{h. c.} \quad (7)$$

Here M_L is the W_L mass, $x_i = m_i^2/M_L^2$, and $\zeta_i \equiv \zeta_i^{LL} = V_{id}^{L*} V_{is}^L$. The QCD correction factors are $\eta_{cc} = 1.38$, $\eta_{tt} = 0.59$, and $\eta_{ct} = 0.47$ [18], and the phase space factors [17] are

$$S(x) = x \left[\frac{1}{4} + \frac{9}{4(1-x)} - \frac{3}{2(1-x)^2} \right] - \frac{3}{2} \left(\frac{x}{1-x} \right)^3 \ln x, \quad (8a)$$

$$S(x_c, x_t) = x_c \left[\ln \frac{x_t}{x_c} - 3 * \frac{x_t}{4(1-x_t)} \left(1 + \frac{x_t}{1-x_t} \ln x_t \right) \right]. \quad (8b)$$

The effective Hamiltonian in Eq. (7) gives

$$\epsilon_K = \frac{G_F^2 M_L^2 (f_K^2 B_K) m_K}{12\sqrt{2}\pi^2 \Delta m_K} [\eta_{cc} S(x_c) I_{cc} + \eta_{tt} S(x_t) I_{tt} + 2\eta_{ct} S(x_c, x_t) I_{ct}], \quad (9)$$

where $I_{ij} \equiv \text{Im}(\zeta_i \zeta_j)$.

In the LRSM, there are additional contributions to the operator $H_{\Delta S=2}$ in which one or both of the W_L in the box diagram are replaced by the W_R . For the mixing matrices as given by Eq. (5), there are no contributions

from W_R - W_R exchanges, since the factors $\zeta_i^{RR} = V_{id}^{R*} V_{is}^R$ all vanish. On the other hand, the W_L - W_R exchanges give an additional piece $\delta H_{\Delta S=2} \equiv H^{LR}$ to $H_{\Delta S=2}$ [19]:

$$H^{LR} = \frac{2G_F^2 M_L^2}{\pi^2} \left(\frac{g_R}{g_L} \right)^2 \beta_R \sum_{i,j=u,c,t} \zeta_i^{LR} \zeta_j^{RL} J(x_i, x_j, \beta_R) (\bar{d}_R s_L) (\bar{d}_L s_R), \quad (10)$$

where $\zeta_i^{LR} = V_{id}^{L*} V_{is}^R$ and $\beta_R = (M_L/M_R)^2$. Moreover, the loop functions are given by

$$J(x_i, x_j, \beta_R) \equiv \frac{\sqrt{x_i x_j}}{4} [(4\eta_{ij}^{(1)} + \eta_{ij}^{(2)} x_i x_j \beta_R) J_1(x_i, x_j, \beta_R) - (\eta_{ij}^{(3)} + \eta_{ij}^{(4)} \beta_R) J_2(x_i, x_j, \beta_R)], \quad (11)$$

with

$$J_1(x_i, x_j, \beta_R) = \frac{x_i \ln x_i}{(1-x_i)(1-x_i\beta_R)(x_i-x_j)} + (i \leftrightarrow j) - \frac{\beta_R \ln \beta_R}{(1-\beta_R)(1-x_i\beta_R)(1-x_j\beta_R)}, \quad (12a)$$

$$J_2(x_i, x_j, \beta_R) = \frac{x_i^2 \ln x_i}{(1-x_i)(1-x_i\beta_R)(x_i-x_j)} + (i \leftrightarrow j) - \frac{\ln \beta_R}{(1-\beta_R)(1-x_i\beta_R)(1-x_j\beta_R)}. \quad (12b)$$

TABLE II: The non-vanishing mixing-angle factors $X_{ij} = X_{ji} \equiv \text{Im}(\zeta_i^{LR}\zeta_j^{RL}) + (i \leftrightarrow j)$ in $H_{\Delta S=2}^{LR}$.

	X_{uc}	X_{ut}
case I	$-\lambda^2 c \sin \tau$	$-A\lambda^4\{(1-\rho)^2 + \eta^2\}^{1/2} \cdot s \sin(\beta + \phi)$
case II	$-c \sin \tau$	$-A\lambda^2 s \sin \phi$

The $\eta_{ij}^{(1)-(4)}$ are QCD correction factors, whose explicit forms are given in Ref. [19].

The contribution of H^{LR} to ϵ_K is given by terms containing the factors $\text{Im}(\zeta_i^{LR}\zeta_j^{RL})$, which involves parameters from both V^L and V^R . The choices of V^R in Eqs. (5) eliminate the W_L - W_R box diagrams with the (t, t) , (c, t) , (t, c) , and (c, c) quark sides. For leading terms in λ , the non-vanishing mixing angle factors are given in Table II, with (u, t) and (u, c) sides, and the W_L - W_R diagrams are suppressed by m_u/m_t or $m_u m_c/m_t^2$, respectively.

The mixing factors shown in Table II have generic values much larger than their counterparts in the SM, which are suppressed by the factors λ^{10} for (t, t) , $\lambda^6 m_c/m_t$ for (c, t) , or $\lambda^2 m_c^2/m_t^2$ for (c, c) . Hence we see that constraints need to be imposed on them for low mass W_R in order that the experimental value $|\epsilon_K| = (2.28 \pm 0.02) \times 10^{-3}$ not be exceeded. These constraints are readily read off from Table II as [20]:

$$\text{case I : } \quad \tau \approx 0, \quad \phi \approx -\beta. \quad (13a)$$

$$\text{case II : } \quad \tau \approx 0, \quad \phi \approx 0. \quad (13b)$$

The constraint conditions also have solutions which can have π added separately to the values above. The important effects of these extra π choices can be included by allowing θ_R to vary from 0 to π . Taking these constraints and the unitarity condition Eq. (6) into account, Eqs. (5) reduce to

$$V_I^R = e^{i\omega} \begin{pmatrix} 1 & 0 & 0 \\ 0 & c & se^{i\sigma} \\ 0 & -se^{-i\beta} & ce^{i(\sigma-\beta)} \end{pmatrix}, \quad (14a)$$

$$V_{II}^R = e^{i\omega} \begin{pmatrix} 0 & 1 & 0 \\ c & 0 & se^{i\sigma} \\ -s & 0 & ce^{i\sigma} \end{pmatrix} \quad (14b)$$

The case II here is more general than that considered in a previous paper, Ref. [21], since it now has a phase and an angle parameter. The previous case II [21] is

equivalent to the special value $c = 0$ here, with only a phase parameter. The overall phase ω does not appear in the K - \bar{K} or B - \bar{B} diagrams. Thus in the cases there is only one relevant free phase left, which we have taken to be σ . Together with the effective right-handed gauge boson mass M_R and the mixing angle θ_R , we have three more parameters in addition to those in the SM, or two more mixing parameters, to the four in the SM.

For large M_R where the constraints Eqs. (13) are not as stringent, the leading (t, t) LR contributions from Eqs. (5) for B_d and B_s systems still have only one arbitrary phase, $(\sigma - \tau)$, whose variation through all values is included in the form of Eqs. (14), thus maintaining the generality of the analysis without the specific form of Eqs. (14).

V. B^0 - \bar{B}^0 MIXING IN THE LRSM

The mixing effect in the B_q^0 - \bar{B}_q^0 system is given by

$$x_q \equiv \frac{\Delta m}{\Gamma} \Big|_{B_q} = 2\tau_{B_q} |M_{q,12}|, \quad (15)$$

where $q = d$ or s , and $M_{q,12}$ is the dispersive part of the mixing matrix element $\langle B_q^0 | H_{\Delta B=2} | \bar{B}_q^0 \rangle$. The operator $H_{\Delta B=2}$ is similar in form to $H_{\Delta S=2}$. In the SM, it is dominated by the box diagram with two internal t -quarks

$$H_{\Delta B=2} = \frac{G_F^2 M_L^2}{4\pi^2} \eta_{tt} S(x_t) \sum_{q=d,s} (V_{tq}^{L*})^2 (\bar{q}_L b_L) (\bar{q}_L b_L) + \text{h. c.}, \quad (16)$$

where $S(x_t)$ is defined in Eq. (8a) and the QCD correction factor $\eta_{tt} = 0.59$ in this case. Eq. (16) then gives

$$M_{q,12}^{LL} = \frac{G_F^2 M_L^2}{12\pi^2} (f_B^2 B_B) m_B \eta_{tt} S(x_t) (V_{tq}^{L*})^2, \quad (17)$$

where we have used the fact that $V_{tb}^L \approx 1$. The evaluation of the hadronically uncertain factor $f_B^2 B_B$ has been the subject of much work, and recent lattice results are summarized in Ref. [22], giving

$$f_{B_q} B_{B_q}^{1/2} = \begin{cases} 228 \pm 32 \text{ MeV}, & \text{for } q = d, \\ 276 \pm 36 \text{ MeV}, & \text{for } q = s, \end{cases} \quad (18)$$

and also $\hat{B}_K = 0.86 \pm 0.13$.

TABLE III: Values of the QCD-factors $\eta_{ij}^{(a)}$ in $J(x_i, x_j, \beta_R)$.

	$\eta_{cc}^{(a)}$	$\eta_{ct}^{(a)}$	$\eta_{tt}^{(a)}$
$a = 1$	0.61	1.27	1.98
2	0.04	0.27	0.75
3	0.55	1.03	1.93
4	0.45	0.84	1.58

In the LRSM, $H_{\Delta B=2}$ receives additional contribution when one or both of the W_L in the box diagrams are replaced by W_R , just as for $H_{\Delta S=2}$ in the K - \bar{K} system. As a result we can write

$$M_{q,12} = M_{q,12}^{LL} + M_{q,12}^{LR} + M_{q,12}^{RR}, \quad (19)$$

where the element $M_{q,12}^{RR}$ is essentially the same as $M_{q,12}^{LL}$ as given by Eq. (17) but with the replacement $L \rightarrow R$ everywhere (and of course we must retain V_{tb}^R , which need not equal to 1):

$$M_{q,12}^{RR} = \frac{G_F^2 M_L^2}{12\pi^2} \left(\frac{g_R}{g_L}\right)^4 (f_B^2 B_B) m_B \beta_R \eta_{tt} S(x_{tR}) \cdot (V_{tq}^{R*} V_{tb}^R)^2, \quad (20)$$

where $x_{tR} = (m_t/M_R)^2$. In case I, this vanishes in B_d - \bar{B}_d mixing because $V_{td}^R = 0$, but it has a contribution to B_s - \bar{B}_s mixing due to the non-zero values of V_{ts}^R and V_{tb}^R . In case II, this contributes to B_d - \bar{B}_d mixing, but vanishes for B_s - \bar{B}_s mixing since $V_{ts}^R = 0$ there.

On the other hand, the matrix element $M_{q,12}^{LR}$ is

$$M_{q,12}^{LR} = \frac{G_F^2 M_L^2}{2\pi^2} \left(\frac{g_R}{g_L}\right)^2 (f_B^2 B_B) \left(\frac{m_B}{m_b}\right)^2 m_B \beta_R \cdot \sum_{i,j=u,c,t} \xi_{q,i}^{LR} \xi_{q,j}^{RL} J(x_i, x_j, \beta_R), \quad (21)$$

where $\xi_{q,i}^{LR} = V_{iq}^{L*} V_{ib}^R$, $\xi_{q,j}^{RL} = V_{jq}^{R*} V_{jb}^L$, and the function $J(x_i, x_j, \beta_R)$ is defined in Eqs. (11)–(12). The QCD-factors $\eta_{ij}^{(1)-(4)}$ in $J(x_i, x_j, \beta_R)$, like all RG correction factors, depend on the relevant mass scales only logarithmically, and hence are relatively insensitive to changes of these masses. Their values at $M_R = 2.5$ TeV and $m_t = 175$ GeV, at the scale $\mu = 4.5$ GeV, are given in Table III [23]. These will be the values we use for subsequent analyses. We also calculate plots for the left-right symmetry limit $g_R = g_L$.

In the summation in Eq. (21), only terms which involve at least one t quark need be considered, mainly due to the quark mass factors $\sqrt{x_i x_j}$. The other terms amount to at most 10^{-3} in magnitude relative to these dominant terms.

To statistically weight the V^L [24] and V^R matrix elements angles s_{23} , s_{13} , and s , and phases δ and σ , we apply six present experimental values, which are those for $|V_{cb}|$, $|V_{ub}/V_{cb}| = 0.087 \pm 0.017$, ϵ_K in the neutral

K system, B_d - \bar{B}_d mixing with ΔM_{B_d} , (which are listed in Table I), as well as the probability of each calculated x_s from the LEPBOSC data average [25], and $\sin 2\beta$ as given in Eq. (4). Complete sets of V^L and V^R angles s_{23} , s_{13} , s , and phases δ and σ are generated, and the results of fitting the experiments are evaluated for each set using χ^2 [26]. χ^2 is formulated as

$$\chi^2 = \sum_i \frac{(f_i(s_{23}, s_{13}, \delta, s, \sigma) - \langle f_i \rangle)^2}{\sigma_i^2}, \quad (22)$$

where $\langle f_i \rangle$ and σ_i are the experimental central values and deviations for $|V_{cb}|$, $|V_{ub}/V_{cb}|$, ϵ_K , ΔM_{B_d} , $\sin 2\beta$, and in $1 - A$ for each calculated x_s , and $f_i(s_{23}, s_{13}, \delta, s, \sigma)$ are the corresponding values evaluated in the LRSM cases.

VI. THE SIZE OF THE LRSM CONTRIBUTIONS TO B MIXING

A. B_d systems

In case I, the loop functions in the W_L - W_R box diagrams as given by Eq. (21) are, like their SM counterparts, increasing functions of the quark masses. Due to the vanishingly small mass of the u quark, only contributions from the c - and t -exchanges need be considered. It turns out that, for V_I^R of the form as given in Eq. (5a), the mixing angle factors $\xi_{d,c}^{RL}$ and $\xi_{d,t}^{RL}$ both vanish. Hence there is essentially no effect of W_R on B_d - \bar{B}_d mixing in case I.

In case II, there is a strong leading W_L - W_R box diagram with a (t, t) pair of t quark exchanges, with $\xi_{d,t}^{LR} \xi_{d,t}^{RL} = A\lambda^2(1 - \rho + i\eta)(-cs)e^{i(\sigma - \tau)}$, with phase $(\beta + \sigma - \tau)$, from Eq. (5b). That is followed by a (c, t) pair of order $m_t m_c \lambda$ whose coefficients are thus about $1/6$ of the leading (t, t) term. We thus have $M_{d,12}^{LR} \sim M_{d,12}^{LL}$ at low M_R . χ^2 contours for the ratio of the LR contribution $|M_{d,12}^{LR}|$ from a W_L - W_R pair over the SM contribution $|M_{d,12}^{LL}|$ as a function of M_R are presented in Fig. 1 for case II. The upper 1 - σ , 90% CL, and 2 - σ contours show the largest LR contributions that still fit the six experimental constraints with one degree of freedom for the three SM V^L and two LR V^R parameters, at $\chi^2 = 1.0$, $\chi^2 = 2.71$, and $\chi^2 = 4.0$, respectively. We see that the right-handed gauge boson W_R can contribute nearly as much to the B_d - \bar{B}_d mixing as the SM for M_R out to at least 12 TeV. In case II, the lower limit on M_R is 600 GeV from a large $120^\circ \leq \delta \leq 160^\circ$ region, and 900 GeV from the normal $40^\circ \leq \delta \leq 80^\circ$ region. The V^R mixing angle θ prefers regions around 0° , 90° , and 180° below 4 TeV, where the leading (t, t) contribution is smaller. All values of the V^R phase σ are allowed above 2 TeV, while $\sigma \leq 180^\circ$ is allowed below 2 TeV.

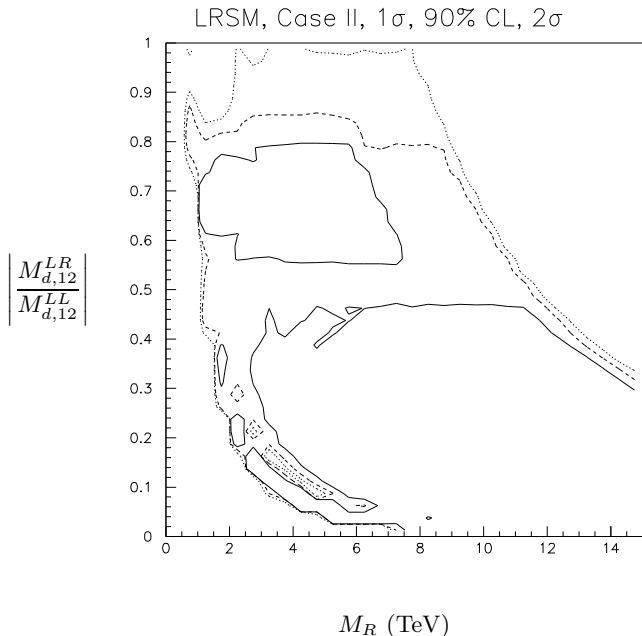


FIG. 1: Plot of $|M_{d,12}^{LR}/M_{d,12}^{LL}|$ as a function of M_R for case II

B. B_s systems

In B_s - \bar{B}_s box diagrams for case I, in $M_{s,12}^{LR}$, four terms from (t, t) , (c, t) , (t, c) and (c, c) pairs contribute. They are dominated by the (t, t) pair, with $\xi_{s,t}^{LR}\xi_{s,t}^{RL} = A\lambda^2 c s e^{i(\sigma-\tau)}$. The χ^2 contours (again, for one degree of freedom) for the scaled ratio $|M_{s,12}^{LR}|/(|M_{s,12}^{LL}| + |M_{s,12}^{LR}|)$ is presented in Fig. 2 for M_R in the range of 0 to 10 TeV. This gives $M_{s,12}^{LR} \sim M_{s,12}^{LL}$ for $M_R \leq 2.5$ TeV, and $M_{s,12}^{LR} \sim 0.1M_{s,12}^{LL}$ for $M_R = 10$ TeV. The W_R contribution to B_s - \bar{B}_s mixing cannot be ignored if $M_R \leq 5$ TeV. Although two W_R 's also appear in the B_s - \bar{B}_s box diagrams for case I, with $(V_{ts}^{R*}V_{tb}^R)^2 = s^2 c^2 e^{2i(\sigma-\tau)}$, their effect is small due to the extra $\beta_R S(x_{tR})$ factor. In case I, the lower M_R limit is about 100 GeV. All σ is allowed. All θ are allowed down to 500 GeV, and below that, the regions around 0° and 180° are preferred.

In case II, the (t, t) , (t, c) , (c, t) , and (c, c) contributions vanish from the structure of Eq. (5b). The leading non-vanishing term in $M_{s,12}^{LR}$ comes from the (t, u) pair, which is suppressed from the SM contribution by $\lambda m_u/m_t$. W_R thus gives no effective contribution to B_s - \bar{B}_s mixing in case II.

VII. CP VIOLATING ASYMMETRY $\sin 2\beta$ IN B^0 DECAYS

The time dependent CP violating phase in $B \rightarrow \psi K_S$ decays is related to the mixing matrix element $M_{d,12}$ and

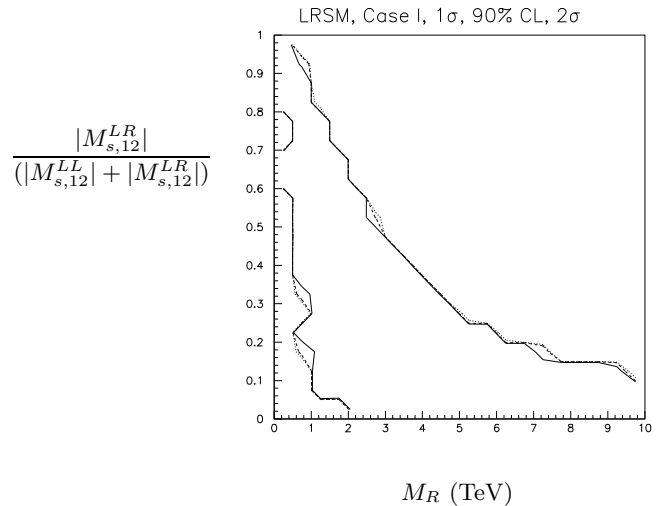


FIG. 2: Plot of $|M_{s,12}^{LR}|/(|M_{s,12}^{LL}| + |M_{s,12}^{LR}|)$ as a function of M_R for case I

the decay amplitudes as follows [16],

$$\sin 2\beta \equiv -\text{Im} \left[\frac{M_{d,12}^* A(\bar{B} \rightarrow \Psi K_S)}{|M_{d,12}| A(B \rightarrow \Psi K_S)} \right]. \quad (23)$$

In addition to the tree graphs, the penguin diagrams, dominated by internal top-quarks, also contribute to $B \rightarrow \psi K_S$ decays in case I. The phase for the W_R penguin amplitude, $V_{tb}^R V_{ts}^{R*} = -c s e^{i(\sigma-\tau)}$, is exactly the same as that for the W_R tree amplitude, $V_{cb}^R V_{cs}^{R*} = c s e^{i(\sigma-\tau)}$. In the SM with W_L , the penguin and tree phases are also equal. Accordingly,

$$A(\bar{B} \rightarrow \psi K_S) \propto V_{cb}^L V_{cs}^{L*} (1 - P) + \beta_{gR} V_{cb}^R V_{cs}^{R*} (1 - P'), \quad (24)$$

where $\beta_{gR} \equiv (g_R/g_L)^2 \beta_R$, and P and P' are the ratios of the W_L and W_R penguin contributions over the tree amplitudes, respectively. The first order approximation $P \cong P' \propto \alpha_s \ln(m_t^2/m_c^2)$ is applied to reach the simplification of $P = P'$ [20]. This makes

$$\sin 2\beta = -\text{Im} \left[\frac{M_{d,12}^*}{|M_{d,12}|} \frac{V_{cb}^L V_{cs}^{L*} + \beta_{gR} V_{cb}^R V_{cs}^{R*}}{V_{cb}^{L*} V_{cs}^L + \beta_{gR} V_{cb}^{R*} V_{cs}^R} \right]. \quad (25)$$

In case II, W_R does not contribute to both the tree and penguin diagrams in $B \rightarrow \psi K_S$ due to $V_{cb}^R V_{cs}^{R*} = 0$ and $V_{tb}^R V_{ts}^{R*} = 0$. Therefore, we have

$$\sin 2\beta = -\text{Im} \left[\frac{M_{d,12}^*}{|M_{d,12}|} \frac{V_{cb}^L V_{cs}^{L*}}{V_{cb}^{L*} V_{cs}^L} \right]. \quad (26)$$

For both cases, since $\sin 2\beta$ is a strongly constrained input parameter, the results are largely compatible with that obtained from the SM, whose range for the same data is $0.63 \leq \sin 2\beta \leq 0.82$, and no plot is shown. An earlier study of LRSB effects in $\sin 2\beta$ is in S. Nam [27].

VIII. SIN γ IN B_s DECAYS

Another asymmetry angle in B meson systems is defined from $B_s \rightarrow D_s^+ K^-$ decays as [28]

$$\sin \gamma \equiv \text{Im} \left(\frac{M_{s,12}}{|M_{s,12}|} \frac{A(B_s \rightarrow D_s^+ K^-)}{A(\bar{B}_s \rightarrow D_s^+ K^-)} \right). \quad (27)$$

The penguin contribution is absent in both $B_s \rightarrow D_s^+ K^-$ and $\bar{B}_s \rightarrow D_s^+ K^-$ decays. Because of the LRSM contribution, γ as defined above is no longer an angle of the unitarity triangle.

The contributions from W_R to both decay modes in case I vanish since $V_{ub}^{R*} V_{cs}^R = 0$ and $V_{cb}^R V_{us}^{R*} = 0$. Therefore, the CP asymmetry for this decay mode can be simplified as

$$\sin \gamma = \text{Im} \left(\frac{M_{s,12}}{|M_{s,12}|} \frac{V_{ub}^{L*} V_{cs}^L}{V_{cb}^L V_{us}^{L*}} \bigg/ \left| \frac{V_{ub}^{L*} V_{cs}^L}{V_{cb}^L V_{us}^{L*}} \right| \right). \quad (28)$$

The allowed χ^2 contours for the CP asymmetry $\sin \gamma$ as a function of M_R is shown in Fig. 3 for case I. We see that all values of $\sin \gamma$ are allowed for $M_R \leq 2$ TeV, and that the 1- σ range does not limit itself to the SM range of $0.55 \leq \sin \gamma \leq 0.96$ until $M_R \sim 6$ TeV.

Because W_R can contribute to $\bar{B}_s \rightarrow D_s^+ K^-$ for case II, we have

$$\sin \gamma = \text{Im} \left(\frac{M_{s,12}}{|M_{s,12}|} \frac{V_{ub}^{L*} V_{cs}^L}{V_{cb}^L V_{us}^{L*} + \beta_{gR} V_{cb}^R V_{us}^{R*}} \bigg/ \left| \frac{V_{ub}^{L*} V_{cs}^L}{V_{cb}^L V_{us}^{L*} + \beta_{gR} V_{cb}^R V_{us}^{R*}} \right| \right). \quad (29)$$

The $\sin \gamma$ values allowed in case II range from 0.64 \rightarrow 0.95 at 1- σ above $M_R = 7$ TeV, with a wider 1- σ region extending down to $\sin \gamma \geq 0.4$ for M_R up to 7 TeV (graph not shown), which comes from a large $125^\circ \leq \delta \leq 160^\circ$ region..

IX. THE SIN 2α ASYMMETRY IN $B_d \rightarrow \pi\pi$

Measurement on the asymmetry in $B_d \rightarrow \pi\pi$ can provide the other CP asymmetry, namely [16],

$$\sin 2\alpha \equiv -\text{Im} \left[\frac{M_{d,12}^*}{|M_{d,12}|} \frac{A(\bar{B} \rightarrow \pi\pi)}{A(B \rightarrow \pi\pi)} \right]. \quad (30)$$

In case I, there is no right handed tree nor penguin diagram for $B_d \rightarrow \pi\pi$ since $V_{ub}^R V_{ud}^{R*} = 0$, $V_{cb}^R V_{cd}^{R*} = 0$, and $V_{tb}^R V_{td}^{R*} = 0$. On the other hand, the penguin pollution for this decay mode in the SM can be removed by isospin analysis [30]. Consequently, we have

$$\sin 2\alpha = \text{Im} \left(\frac{M_{d,12}^*}{|M_{d,12}|} \frac{V_{ud}^{L*} V_{ub}^L}{V_{ud}^L V_{ub}^{L*}} \right). \quad (31)$$

In case II, there are right handed W_R penguin diagrams for $B_d \rightarrow \pi\pi$ from $b \rightarrow d$ through virtual t and c quarks.

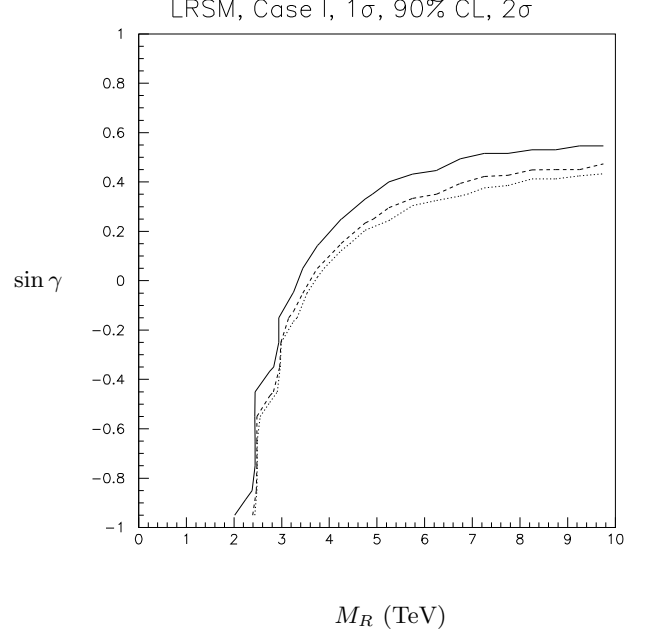


FIG. 3: Plot of $\sin \gamma$ as a function of M_R for case I

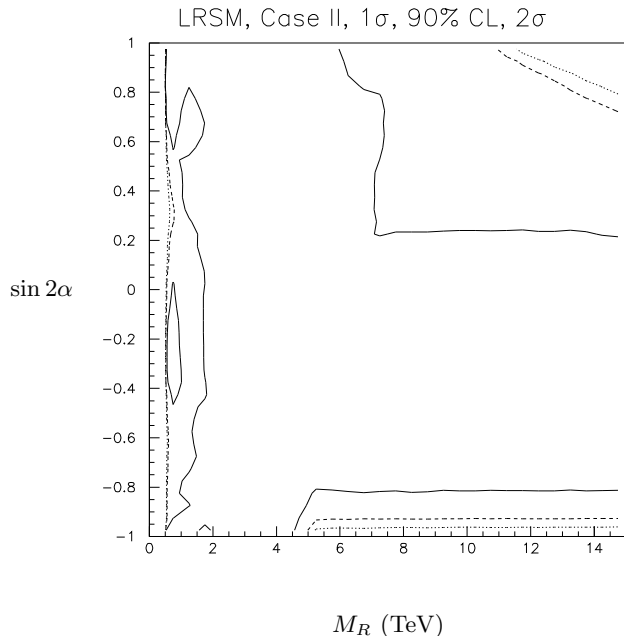
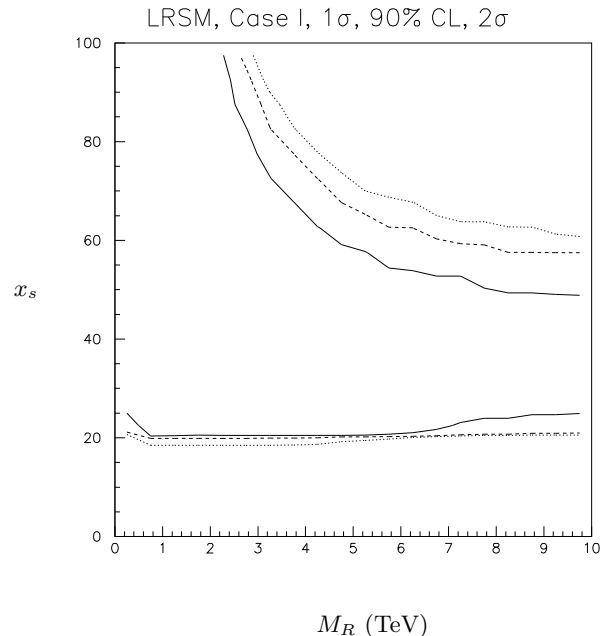
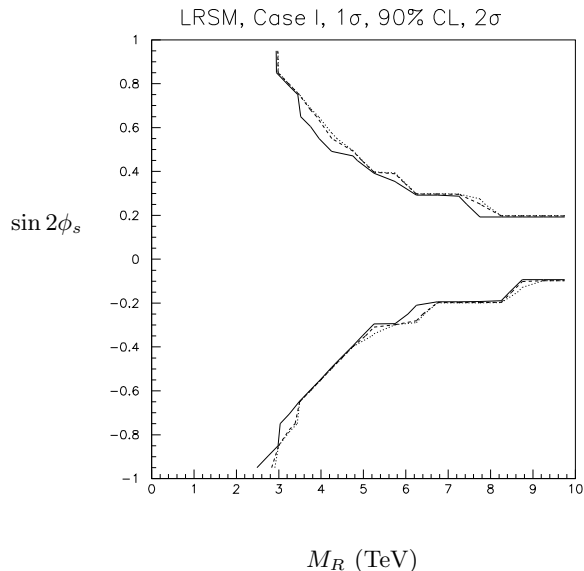
The mixing product for these two processes, which are given in $V_{tb}^R V_{td}^{R*} = -cse^{i(\sigma-\tau)}$ and $V_{cb}^R V_{cd}^{R*} = cse^{i(\sigma-\tau)}$, respectively, are equal and opposite, but the amplitudes do not cancel since m_t and m_c are different. They are included with the W_L penguins to be isolated by isospin analysis. We note that the right handed penguins might be appreciable since the left handed penguins are suppressed by Λ^3 . There is no right handed tree diagram in this case since $V_{ub}^R = 0$. We still use Eq. (31) to calculate for case II, although again, α is not the angle in the unitarity triangle in the LRSM. Fig. 4 shows the χ^2 contours for $\sin 2\alpha$ from -1 up to 1 for $M_R \leq 7$ TeV in case II, and approximating the 1- σ SM range for $\sin 2\alpha$ of $-0.9 \leq \sin 2\alpha \leq 0.33$ for larger M_R . There is a large $125^\circ \leq \delta \leq 160^\circ$ region that contributes out to 7 TeV. The positive $\sin 2\alpha$ region results from the larger δ region where $\alpha \leq 90^\circ$ and $2\alpha \leq 180^\circ$.

X. THE SIN $2\phi_s$ ASYMMETRY IN B_s MIXING

The mixing in B_s - \bar{B}_s is the same as $\sin 2\phi_s$, where ϕ_s is the small angle in the SM (b - s) unitarity triangle. Since this involves B_s mixing, it only appears in case I, and is given by [21]

$$\sin 2\phi_s = -\text{Im} \left(\frac{M_{s,12}}{|M_{s,12}|} \frac{V_{cb}^{L*} V_{cs}^L + \beta_{gR} V_{cb}^{R*} V_{cs}^R}{V_{cb}^L V_{cs}^{L*} + \beta_{gR} V_{cb}^R V_{cs}^{R*}} \right). \quad (32)$$

Here, W_R can also contribute to $\bar{b} \rightarrow \bar{c}\bar{s}$ decays. In the LRSM, with the asymmetry defined as above, ϕ_s is no longer the angle in the V^L unitarity triangle. The

FIG. 4: Plot of $\sin 2\alpha$ as a function of M_R for case IIFIG. 6: Plot of x_s as a function of M_R for case IFIG. 5: Plot of $\sin 2\phi_s$ as a function of M_R for case I

χ^2 contours for $\sin 2\phi_s$ in case I are shown in Fig. 5 and show $\sin 2\phi_s$ from -1 to 1 for M_R up to 3 TeV, and above the SM range up to 8 TeV. The SM $1\text{-}\sigma$ $\sin 2\phi_s$ range for the same data runs from $0.025 \leq \sin 2\phi_s \leq .041$. This measurement could provide dramatic evidence for new physics.

XI. x_s , THE B_s OSCILLATION RATE

Since x_s measures the B_s oscillation rate, it is only affected in case I. It is given by its ratio to x_d as [21]

$$x_s = 1.034x_d \left| \frac{M_{s,12}}{M_{d,12}} \right|, \quad (33)$$

where $M_{s,12}$ contains the W_R box diagrams, and $x_d = 0.77$.

The χ^2 contours for x_s are shown in Fig. 6 for case I. They show x_s from 20 to greater than 100 for $M_R \leq 2$ TeV. There is no experimental upper limit to x_s . In the LRSM, the order unity V_{ts}^R matrix element for the W_R exchange replaces the SM suppressed $V_{ts}^L = -A\lambda^2 = -0.04$ matrix element, giving low mass W_R an initial advantage. The SM $1\text{-}\sigma$ range is $24 \leq x_s \leq 53$, which is approached for case I for M_R above 5 TeV.

XII. CONCLUSIONS

In the Left-Right Symmetric Model, the right-handed quark mixing matrices can be parametrized into two cases as described in Eqs. (5), which provide a reasonable lower limit for the W_R mass [14]. We suppress the large contributions to ϵ_K from the W_L - W_R box diagram by effectively taking some parameters of V^R to vanish, as shown in Eqs. (14), so that the quite small experimental value of ϵ_K can be achieved and W_R may give the most substantial effects on CP asymmetries in B decays [20] [21].

In this paper we have given the detailed calculations, as a function of M_R , of the total mixing matrix element $M_{q,12}$ and of its components $M_{q,12}^{LL}$, $M_{q,12}^{RR}$ and $M_{q,12}^{LR}$, where two W_L , two W_R and a W_L - W_R pair are exchanged in the box diagrams, for both B_d and B_s systems. The effects of W_R are depicted by the ratios $|M_{q,12}^{LR}|/|M_{q,12}^{LL}|$ in both B_d - \bar{B}_d and B_s - \bar{B}_s mixing, which are plotted in Figs. 1 and 2 for cases II and I, respectively. In case I the LRSM shows significantly larger allowed regions for $M_R \leq 6$ TeV in B_s oscillation related x_s and $\sin \gamma$, and beyond for $\sin 2\phi_s$. It effects B_d asymmetries out to 1

TeV. In case II, the second quadrant δ region can affect the unitarity triangle angles and its vertex for $M_R \leq 8$ TeV in the LRSM. It also affects $\sin 2\phi_s$ and x_s at 90% CL beyond 8 TeV.

Whereas $\sin 2\beta$ as a function of M_R is compatible with that obtained from the SM, much larger allowed regions for $\sin \gamma$, $\sin 2\alpha$, x_s , and $\sin 2\phi_s$ are found when the LR amplitudes are large, as stated above.

Consequently, measurements of the additional CP violating asymmetries beyond $\sin 2\beta$ can provide interesting tests for the new physics given by the LRSM.

-
- [1] R. Mohapatra and J. Pati, Phys. Rev. D 11, 566 (1975), 2558 (1975); R. Mohapatra and G. Senjanovic, Phys. Rev. D 12, 1502 (1975).
- [2] K. Hagiwara *et al.*, Phys. Rev. D 66, 010001-1(2002).
- [3] A. B. Carter and A. I. Sanda, Phys. Rev. Lett. 45, 952 (1980); Phys. Rev. D 23, 1567 (1981).
- [4] N. Cabibbo, Phys. Rev. Lett. 10, 531 (1963); M. Kobayashi and T. Maskawa, Prog. Theor. Phys. **49**, 652 (1973).
- [5] L. Wolfenstein, Phys. Rev. Lett. 51, 1945 (1983).
- [6] C. Jarlskog, Phys. Rev. Lett. 55, 1039 (1985).
- [7] T. Caravaglios, F. Parodi, P. Roudeau, and A. Stocchi, *Taipei 1999, B physics and CP violation*, p. 105 (1999), hep-ph/0002171.
- [8] A. Ali and D. London, *Frascati:1999, Physics and Detectors for DAPHNE*, hep-ph/0002167.
- [9] B. Aubert *et al.* (the BaBar Collaboration), Phys. Rev. Lett. 89, 201802 (2002).
- [10] K. Abe *et al.* (the Belle Collaboration), Phys. Rev. D 66, 071102 (2002).
- [11] T. Affoler *et al.*, Phys. Rev. D 61, 072005 (2000).
- [12] G. Beall, M. Bander, and A. Soni, Phys. Rev. Lett. 48, 848 (1982).
- [13] F. I. Olness and M. E. Ebel, Phys. Rev. D 30, 1034 (1984).
- [14] P. Langacker and S. Sankar, Phys. Rev. D 40, 1569 (1989).
- [15] D. London and D. Wyler, Phys. Lett. **B232**, 503 (1989).
- [16] Y. Nir and H. Quinn, in *B decays*, edited by S. Stone (World Scientific, Singapore, 1994), p. 362; A. Dar, G. Eilam, and M. Gronau, Nucl. Phys. B (Proc. Suppl.) **38**, 136 (1995).
- [17] A. Buras, W. Slominski, and H. Steger, Nucl. Phys. **B238**, 529 (1984); T. Inami and C. Lim, Prog. Theor. Phys. **65**, 297 (1981).
- [18] S. Herrlich and U. Nierste, Nucl. Phys. **B419**, 292 (1994); Phys. Rev. D 52, 6505 (1995); A. Buras, M. Jamin, and P. Weisz, Nucl. Phys. **B347**, 491 (1990).
- [19] G. Ecker and W. Grimus, Nucl. Phys. **B258**, 328 (1985); H. Nishiura, E. Takasagi, and M. Tanaka, Prog. Theor. Phys. **84**, 116 (1990); **85**, 343 (1991).
- [20] T. Kurimoto, A. Tomita, and S. Wakaizumi, Phys. Lett. **B381**, 470 (1996).
- [21] D. Silverman and H. Yao, J. High Ener. Phys. **0110**, 008 (2001).
- [22] D. Becirevic, XXXVIII Rencontres de Moriond, Les Arcs, France, (2003).
- [23] H. Yao, Chin. J. Phys. **32**, 96 (1994).
- [24] K. Hagiwara *et al.* (Particle Data Group), Phys. Rev. D 66, 010001 (2002).
- [25] *The LEP B Oscillations Working Group*, http://lepbose.web.cern.ch/LEPBOSC/combined_results/lathuile_2003/, LEPBOSC 98/3 (1998), updated for the LaThuile and Moriond conferences, 2003.
- [26] D. Silverman, Int. J. Mod. Phys. **A13**, 2253 (1996); D. Hawkins and D. Silverman, Phys. Rev. D 66, 016008 (2002).
- [27] S. Nam, Phys. Rev. D 66, 055008 (2002).
- [28] R. Aleksan, I. Dunietz, B. Kayser and F. Le Diberder, Nucl. Phys. B **361**, 141 (1991); R. Aleksan, I. Dunietz and B. Kayser, Z. Phys. C **54**, 653 (1992).
- [29] A. Stocchi, Nucl. Instrum. Meth. A462: 318 (2001), hep-ph/0012215.
- [30] M. Gronau and D. London, Phys. Rev. Lett. 65, 3381 (1990); H. Lipkin, Y. Nir, H. Quinn and A. Snyder, Phys. Rev. D 44, 1454 (1991); M. Gronau, O. Hernandez, D. London and J. Rosner, Phys. Rev. D 52, 6374 (1995).